Thermal conductivity of multiwalled carbon nanotubes

Da Jiang Yang, Qing Zhang, George Chen, S. F. Yoon, J. Ahn, S. G. Wang, Q. Zhou, Q. Wang, and J. Q. Li
Microelectronics Centre, School of Electrical and Electronic Engineering, S1-B2c-20, Nanyang Avenue, Nanyang Technological University, 639798, Singapore

(Received 30 April 2002; revised manuscript received 19 August 2002; published 31 October 2002)

Thermal conductivity of multiwalled carbon nanotubes (CNT's) prepared using a microwave plasma chemical vapor deposition system is investigated using a pulsed photothermal reflectance technique. We find that the average thermal conductivity of carbon nanotube films, with the film thickness from 10 to 50 μm, is around 15 W/m K at room temperature and independent of the tube length. Taking a small volume filling fraction of CNT's into account, the effective nanotube thermal conductivity could be 2×10^2 W/m K, which is smaller than the thermal conductivity of diamond and in-plane graphite by a factor of 9 and 7.5, respectively.

DOI: 10.1103/PhysRevB.66.165440 PACS number(s): 65.80.+n

I. INTRODUCTION

A carbon nanotube (CNT) is a type of very attractive material for many unique properties because of its nanometer size tubular structure. Extremely high thermal conductivity is theoretically predicted for CNT's, due to large phonon mean free path in strong carbon sp^2 bond network of CNT walls.[1] Che *et al.*[2] used equilibrium molecular dynamics to simulate the thermal conductivity of single-walled carbon nanotube (SWNT's) and suggested that it is dependent on the concentration of vacancies and defects in the CNT's. Theoretical value of it approaches 2980 W/m K along the tube axis, which is even higher than that of good conventional thermal conductors, such as diamond.

So far, some experimental results of thermal conductivity for single-walled and multiwalled carbon nanotubes (MWNT's) have been reported.[3–7] However the values deviate each other very largely, from 20 to 3000 W/m K. The measurement techniques include comparative method[3] and 3 ω method.[8] Although these studies provide considerable knowledge of heat transport along CNT's, some problems still need clarifying. First, previously measured thermal conductivity of bulk CNT's may not reflect intrinsic CNT thermal conductivity due to the effect of volume filling fraction. Secondly, for a steady-state method, radiative heat loss could lead to an uncertainty of determining the thermal conductivity. Finally, in practical CNT electronic applications, such as CNT based transistors, photodetectors, bio/chemical sensors etc., CNT length dependence of thermal conductivity will be considered as one of a few key factors in design. However, the relevant results have not been reported yet.

In this paper, we present the thermal conductivity of MWNT films measured by a pulsed photothermal reflectance (PPR) technique. In this noncontact technique, sample preparation is relatively simple. Most importantly, one can treat the heat conduction problem as one dimensional and heat generation as surface heating.[9] Moreover, heat loss can be neglected due to the short time ($\sim$400 μs) of the measurement.

II. EXPERIMENTAL DETAILS

Groove structures are chemically etched on high resistivity silicon (100) substrates. The depth and width of the structure are 10–50 μm and 3–5 mm, respectively. Nickel thin films with thickness ranging from 0.5 to 100 nm are selectively deposited on the groove structured silicon substrates. The Ni films in the groove structures serve as catalyst for growing CNT's in $CH_4+H_2+N_2$ microwave plasma. Substrate temperature, reactant gas flow ratio of $H_2:CH_4:N_2$, microwave power, deposition pressure, and deposition time are 720 °C, 200:20:10 sccm, 1300 W, 35 Torr, and 10 min, respectively. The length of the MWNT's ranges from 10 to 50 μm and the diameter is from 40 to 100 nm. To enhance heat absorption in our PPR measurement, 1.2-μm thick gold foil is closely attached to the top of the CNT films. Procedure of the sample preparation is shown in Fig. 1.

Figure 2 shows the setup of our PPR measurement system. During the measurement, the gold foil is struck by a Nd:YAG laser pulse with a pulse width [full width at half maximum (FWHM)] of 8 ns, spot size of 3 mm, pulse energy of 30.3 μJ, and frequency of 10 Hz. Immediately after the laser pulse striking, the sample surface temperature rises sharply and then drops to room temperature. Estimated surface temperature excursion of about 31 K is about 10% of the measuring temperature. The temperature decay time is governed by thermal conduction properties of the CNT film underneath the gold foil. A focused continuous He-Ne laser is reflected from the gold foil surface, probing the light reflection variation of the gold foils. Since the reflectivity is very sensitive to the surface temperature,[10] by inverting the obtained signal, a temperature excursion profile can be obtained. The system was calibrated by measuring the thermal conductivity of silicon dioxide film.

III. RESULTS AND DISCUSSION

We use a three-layer model to simulate heat transport in Au/CNT's/Si structure. For a detailed description about the modeling, refer to previous papers.[11,12] To minimize the effect of thermal transport through intertube airspace, the effective thermal conductivity is deduced from the difference in the temperature profiles of Au/CNT's/Si and Au/airgap/Si.

Figure 3 shows the normalized surface temperature profiles for location A ‘‘Au/airgap/Si’’ and location B ‘‘Au/CNT's/Si,’’ respectively. To obtain the thermal conductivity of CNT's, the temperature profile is fitted using a three-layer

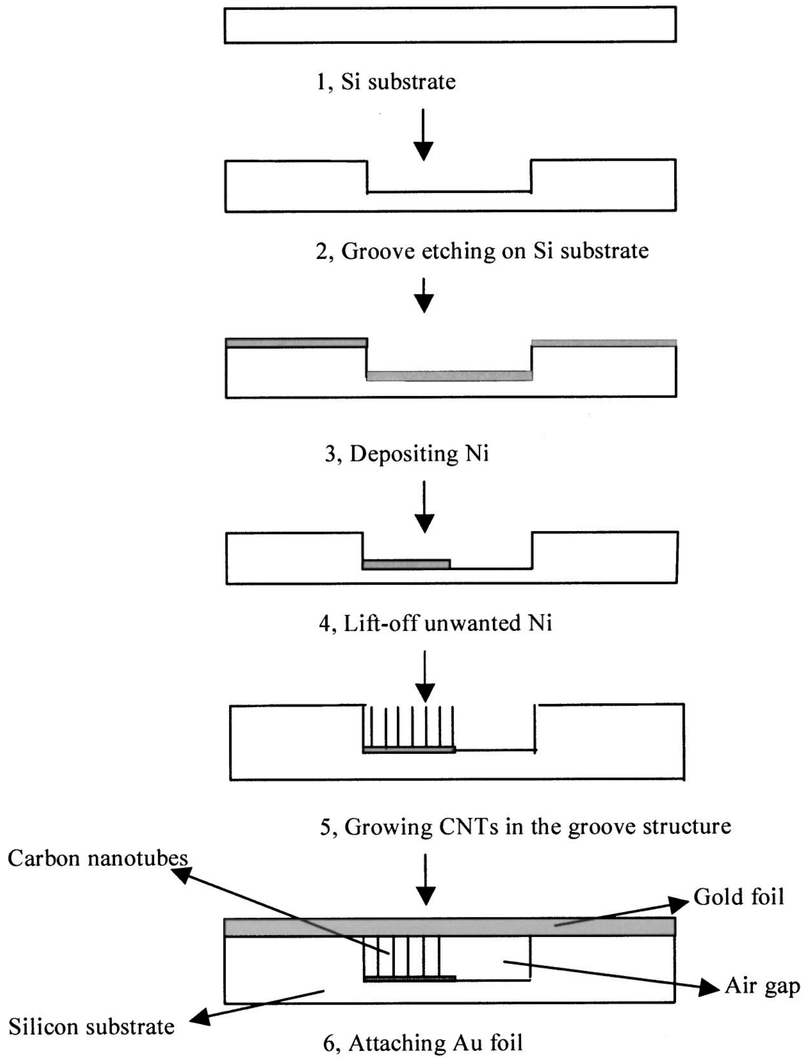

FIG. 1. Procedures of the CNT samples preparation.

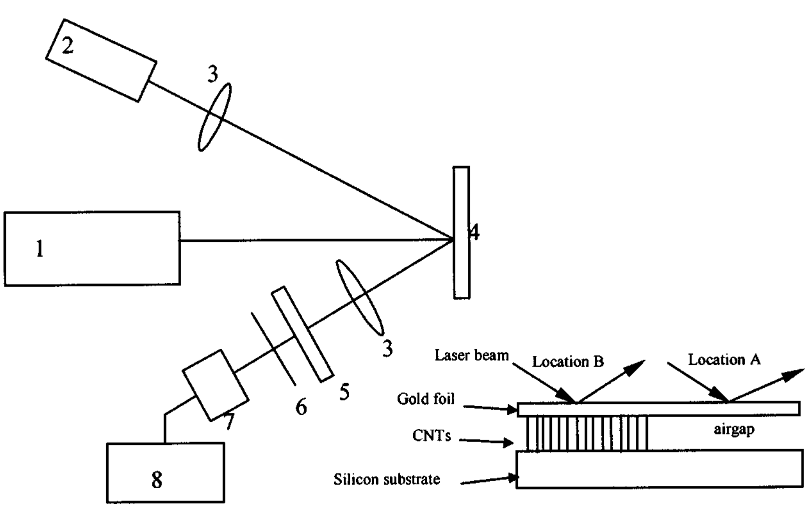

FIG. 2. Photothermal reflection experiment setup. (1) Pump Nd:YAG laser, (2) probe He-Ne laser, (3) lens, (4) sample, (5) attenuator, (6) filter, (7) photodetector, (8) oscilloscope. Inset: Cross-section schematic illustration of CNT samples used in the measurement.

heat conduction model. The silicon substrate is modeled as an infinite medium, because heat diffusion length in silicon is 3.7×10^{-4} m,[13] which is less than the thickness of silicon substrate. The Laplace transform of surface temperature profile $T(s)$ can be described by

$$T(s)=\frac{Q(s)}{e_1\sqrt{s}}\left[\frac{(\cosh\eta_2\sqrt{s}+e_{32}\sinh\eta_2\sqrt{s})\cosh\eta_1\sqrt{s}+(e_{31}\cosh\eta_2\sqrt{s}+e_{21}\sinh\eta_2\sqrt{s})\sinh\eta_1\sqrt{s}}{(e_{31}\cosh\eta_2\sqrt{s}+e_{21}\sinh\eta_2\sqrt{s})\cosh\eta_1\sqrt{s}+(\cosh\eta_2\sqrt{s}+e_{32}\sinh\eta_2\sqrt{s})\sinh\eta_1\sqrt{s}}\right], \quad (1)$$

where $e_i=\sqrt{\rho_i C_i K_i}$, $e_{ij}=e_i/e_j$, $\eta_i=d_i/\sqrt{\alpha_i}$, $i=1,2,3$. Subscripts 1, 2, and 3 stand for the Au foil, CNT's or airgap and silicon substrate, respectively. ρ, C, K, e, α, and d are the bulk density, specific heat, thermal conductivity, thermal effusivity, thermal diffusivity, and thickness of each layer, respectively. $Q(s)$ is the Laplace transform of the Nd:YAG laser pulse, in a form of

$$Q(s)=\frac{1}{2}\left[1+\mathrm{Erf}\left(\frac{b}{g}-\frac{gs}{2}\right)\right]\exp\left[-bs+\frac{1}{4}g^2s^2\right], \quad (2)$$

where $b=2.0\times10^{-6}$ s and $g=5.764\times10^{-9}$ s for the laser pulse we used.

In order to fit the temperature excursion profile, Eq. (1) is inversely Laplace transformed into time domain using Stehfest numerical method.[14] The bulk density of 1.93×10^4 kg/m^3 and specific heat of 129 J/kg K for Au are used in the fitting.[15] The thermal conductivity for silicon substrate is taken as 148 W/m K.[13] Fitting parameters are the thermal conductivities of Au foil and CNT films, and the thermal diffusivity of the CNT films. One can see that the simulated curves fit the measured temperature profiles reasonably well for 40-μm thick airgap [Fig. 4(a)] and CNT film, [Fig. 4(b)]. The average fitted thermal conductivity of the CNT film is about 15 W/m K. We have measured CNT films with different thickness from 10 to 50 μm, and the fitted values are listed in Table I. It is found that the thermal conductivity for the four CNT films ranged from 12 to 17 W/m K. The variation range of the fitted thermal conductivity depends on the signal to noise ratio. One can see that the thermal conductivity does not show a CNT film thickness dependence. In other words, it is independent of the length of CNT's. The fitted thermal conductivity for airgap is around 0.0264 W/m K, consistent with the literature value of 0.026 W/m K. It is also noticed that the average thermal conductivity of Au foil is about 260 W/m K, only about 80% of Au bulk value. Hartmann[16] have confirmed that thermal conductivity of Au film is strongly dependent on the film thickness due to the influence of surface and grain boundary scattering. In addition, voids and microcracks within the gold foil may also reduce thermal conductivity efficiently.[17]

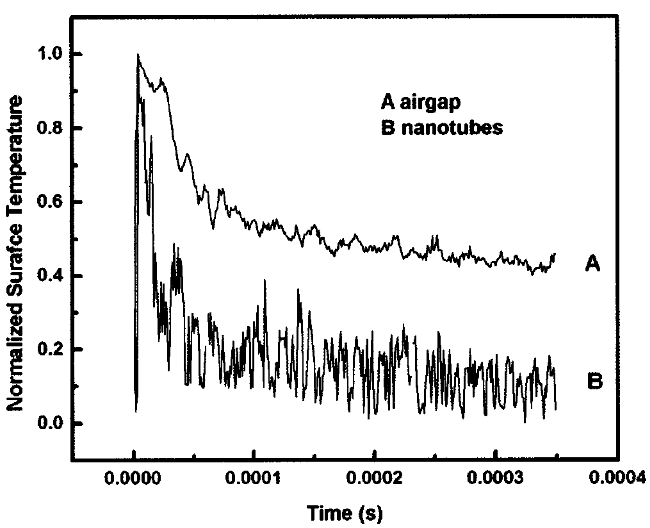

FIG. 3. Four-point smoothed Transient surface temperature profiles of 40-μm thick CNT film and the air gap.

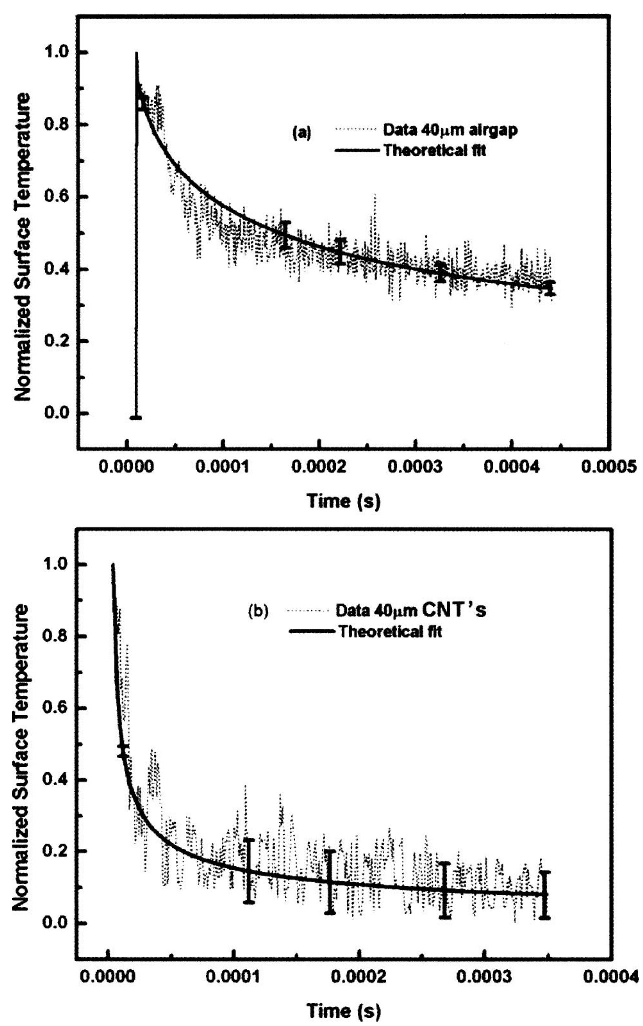

FIG. 4. Measured and fitted temperature profiles for 40-μm thick (a) airgap and (b) CNT film.

TABLE I. Thermal properties vs thickness of CNT samples.

Tube length (μm)	12	25	40	46
K_{Au} (W/m K)	268–288	182–243	267–295	250–310
K_{tube} (W/m K)	13–17	12–16.5	13–17	14–17
Thermal diffusivity $\alpha_{\mathrm{tube}}(10^{-5}\ \mathrm{m^2\,s^{-1}})$	1–2.6	1–10	5–9	0.7–1

Contact thermal resistance between the gold foil and CNT's does not affect our CNT thermal conductivity very much. With our CNT's length 10–50 μm and CNT thermal conductivity of 12–17 W/m K, the sample thermal resistance could be $0.8\text{–}2.9\times10^{-6}\ \mathrm{m^2\,K/W}$, which is contributed by both CNT thermal resistance and the contact thermal resistance. Figure 5 shows how the thermal resistance varies as a function of the thickness of CNT films. A contact thermal resistance of $2.2\times10^{-8}\ \mathrm{m^2\,K/W}$ is obtained by extrapolating the nice linear fitting to zero film thickness and it is one or two orders of magnitude smaller than the CNT thermal resistance. Therefore the contact thermal resistance can be ignored. In addition, the boundary thermal resistance caused by acoustic mismatch is even one order of magnitude smaller than the obtained contact thermal resistance.[18] Thus, contribution from acoustic mismatch is negligible as well.

Heat loss in the measurement also does not affect the obtained thermal conductivity. First, it has been found that, in transient thermal conductivity measurement by a flash technique, the heat loss is noticeable when the temperature decay time is more than 30 ms or 5 s,[12,19] respectively. In our measurement, the temperature rise is 20–30 K above the environment temperature (room temperature) and the temperature excursion duration is only ~400 μs. By comparing our experimental conditions with those used in flash technique,[12,19] we suggest that the radiative heat loss in our measurement is not significant. Second, using the three layer model described in the text, the surface temperature of gold foil $T^*(s)$ with heat loss will be

$$T^*(s)=Q(s)\left\{\frac{(\cosh\eta_2\sqrt{s}+e_{32}\sinh\eta_2\sqrt{s})\cosh\eta_1\sqrt{s}+(e_{31}\cosh\eta_2\sqrt{s}+e_{21}\sinh\eta_2\sqrt{s})\sinh\eta_1\sqrt{s}}{\left[\begin{array}{l}[(e_{31}\cosh\eta_2\sqrt{s}+e_{21}\sinh\eta_2\sqrt{s})\cosh\eta_1\sqrt{s}+(\cosh\eta_2\sqrt{s}+e_{32}\sinh\eta_2\sqrt{s})\sinh\eta_1\sqrt{s}]e_1\sqrt{s}\\ +h_{c,r}[(\cosh\eta_2\sqrt{s}+e_{32}\sinh\eta_2\sqrt{s})\cosh\eta_1\sqrt{s}+(e_{31}\cosh\eta_2\sqrt{s}+e_{21}\sinh\eta_2\sqrt{s})\sinh\eta_1\sqrt{s}]\end{array}\right]}\right\},\quad(3)$$

where h_c and h_r are the convective and radiative heat transfer coefficients, respectively. For the case of convective heat loss, according to the definition of h_c,

$$h_c=\frac{-K_{\mathrm{air}}dT/dz}{T},\quad(4)$$

where $T=T_2-T_1$, T_2 is the gold surface temperature with a maximum value of 55 °C, T_1 is the ambient temperature of 25 °C, and dT/dz is the temperature gradient normal to the gold foil. h_c can be evaluated to be 24 $\mathrm{W/m^2\,K}$ using the thermal conductivity of $K_{\mathrm{air}}\sim0.027$ W/m K. Substituting $d_{\mathrm{Au}}=1.2\ \mu$m, $K_{\mathrm{Au}}=240$ W/m K, $e_1=2.16\times10^4\ \mathrm{W\,s^{1/2}\,m^{-2}\,K^{-1}}$, $\eta_1=1.95\times10^{-4}\ \mathrm{s^{1/2}}$, $d_2=40\ \mu$m, $K_{\mathrm{tube}}=15.5$ W/m K, $e_2=1.81\times10^3\ \mathrm{W\,s^{1/2}\,m^{-2}\,K^{-1}}$, $\eta_2=4.82\times10^{-3}\ \mathrm{s^{1/2}}$, $e_3=1.56\times10^4\ \mathrm{W\,s^{1/2}\,m^{-2}\,K^{-1}}$, and $h_c=24\ \mathrm{W/m^{-2}\,K}$ into Eq. (3). Through inverse Laplace transform, the value of $[L^{-1}T^*(s)-L^{-1}T(s)]/L^{-1}T(s)\sim10^{-4}$. This indicates that the influence of the convective heat loss on the gold foil temperature profile can be ignored.

As for the radiation effect, using Au emissivity of $\varepsilon_m=0.07$, the Stefan-Boltzmann constant $\sigma_{\mathrm{SB}}=5.67\times10^{-8}\ \mathrm{W/m^2\,K^4}$, $T_2=329$ K, and $T_1=298$ K, the maximum value of h_r is evaluated as

$$h_r=\varepsilon_m\sigma_{\mathrm{SB}}(T_2^2+T_1^2)(T_2+T_1)=0.49\ \mathrm{W/m^2\,K}.\quad(5)$$

Since $h_r/h_c\sim0.02$, the radiative heat loss should be much smaller than the convective heat loss. Thus, radiative heat loss can be also neglected.

The obtained thermal conductivity of CNT films is not as high as those expected values, as mentioned in the introduction. Let us examine the effect of intertube airspace, which is highly resistive to heat conduction. A thermal conductance model is shown in Fig. 6. The total thermal conductance of the CNT films is contributed from the effective thermal conductance of CNT's and the airgap, i.e.,

$$\frac{K_{\mathrm{tube}}}{d}=\frac{K_{\mathrm{tube}}^*\delta}{d}+K_{\mathrm{air}}\frac{1-\delta}{d},\quad(6)$$

where K_{tube}^* is the effective thermal conductivity for the CNT's, K_{tube} is the fitted thermal conductivity for the CNT film, K_{air} is the thermal conductivity for air. δ is the CNT volume filling fraction and d is the thickness of the tube films or airgap. Through weighing the groove-structured sample before and after CNT's growth and assuming the mass density of MWNT $\rho\sim1.34\ \mathrm{g/cm^3}$, the value of δ is determined to be about 7–8 % for the four samples. By substituting the average values of K_{tube} and K_{air} into Eq. (6), we have $K_{\mathrm{tube}}^*=2\times10^2$ W/m K.

To have a better understanding of the thermal transport in CNT's, other fitting parameters shown in Table I should be

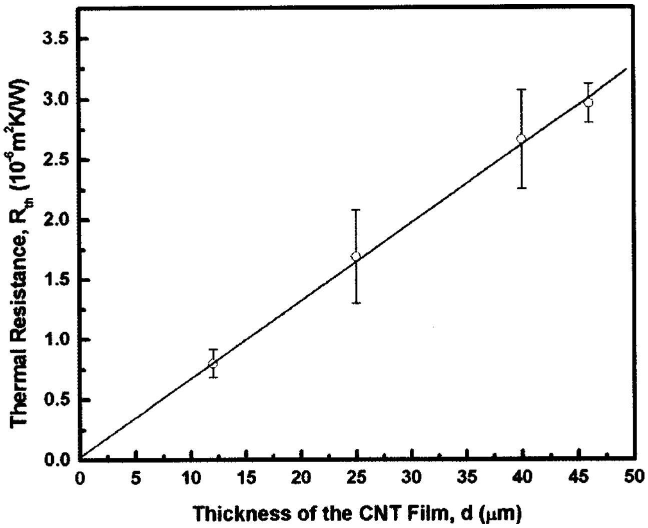

FIG. 5. Thermal resistance of Au/CNT's as a function of the CNT length.

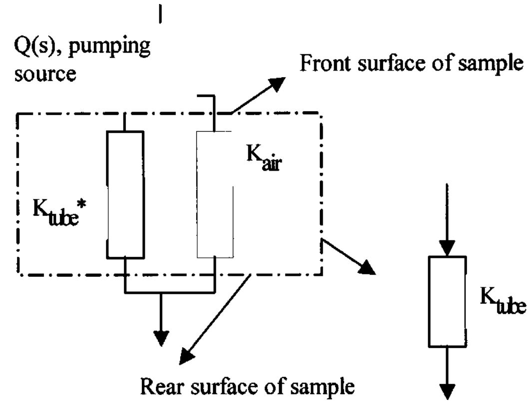

FIG. 6. Schematic illustration for thermal conductance model.

addressed here. One can see that the thermal diffusivity α is diverging with the thickness of the tube films. Using the relation $\alpha \sim K^*/\rho C$ and using the mass density of MWNT $\rho \sim 1.34\ \mathrm{g/cm^3}$, the specific heat C of the MWNT's can be calculated out around $1-7\times 10^3$ J/kg K. This is larger than the published value of 470 J/kg K.[5] Benedict *et al.*[20] predicted that the specific heat could depend on the diameter of CNT's. Phonon dominant specific heat is directly related with the phonon density of state (PDOS). Small diameter CNT's have large strain due to their large curvatures in comparison with large diameter CNT's. This particular strain effect is thought to be the reason for the differences in the PDOS, which will further affect the specific heat. Interestingly, our MWNT diameters distribute from 40 to 100 nm, indeed larger than those CNT's used in the experiment of Yi *et al.*,[5] where the diameters were from 20 to 40 nm.

Electrical conductivity σ of the same tube films is determined to be $1.6–5\times 10\ \Omega^{-1}\,\mathrm{cm}^{-1}$. Using the Wiedemann-Franz law,[21] the ratio of $K/\sigma T$ ($T=300$ K) for our sample is around $1-4\times 10^{-4}\ (\mathrm{V/K})^2$, is the electrical of the CNT samples, which is three or four orders of magnitude larger than the free-electron Lorenz number of $2.45\times 10^{-8}\ (\mathrm{V/K})^2$. Therefore, we suggest that the thermal conductivity of MWNT's is dominantly contributed by phonons, or $K \sim Cvl$, where v is the characteristic sound velocity for CNT's and l is the phonon mean free path. With $K^*_{\mathrm{tube}} = 200$ W/m K and $v = 10^4$ m/s,[7] we have $l \sim 20$ nanometers, which is smaller than that calculated by Kim *et al.*[6] For our MWNT's, due to the large length of our tube samples (10–50 μm), boundary scattering could not be the main reason to reduce the phonon mean free path. Intergraphene layer and intertube coupling as well as the defects scattering are more likely to reduce the phonon mean free path.[1,2,6] This could be the reason why our measured K^*_{tube} is much smaller than the expected value.

Maruyama[22] proposed that thermal conductivity of CNT's may converge when the tube length is much longer than the phonon mean free path. As was confirmed by Che's[2] simulation, if the CNT length is larger than 15 nm, theoretical thermal conductivity converges to a value of 2980 W/m K. In our case, the length of MWNT's ranges from 10 to 50 μm, much far beyond the phonon mean free path of 20 nm. Therefore, the thermal conductivity should not depend on the CNT length for our CNT films. This expectation is confirmed by our measurement, as shown in Table I.

Using equilibrium and nonequilibrium molecular dynamics simulations with accurate carbon potential, Berber[1] predicted the thermal conductivity of (10,10) SWNT of $K \sim 6600$ W/m K at room temperature. In contrast, Maruyama[22] obtained the thermal conductivity of (5,5) SWNT of $K \sim 600$ W/m K at room temperature using phantom technique, ten times smaller than Berber's results. Kim *et al.*[6] through measuring a microfabricated suspended device, determined the thermal conductivity of 3000 W m K for a single MWNT. However, Hone *et al.*[3] measured the thermal conductivity of crystalline ropes of SWNT's and obtained a value of 35 W/m K at room temperature, in the same order of magnitude as the value observed by Yi *et al.*[5] for the bundles of MWNT's. One year later, the former authors reported a value of 200 W/m K for magnetically aligned SWNT film.[4] From above, we can see that for a single tube, either single-walled or multiwalled, the thermal conductivity is from 600 to 6000 W/m K, significantly higher than the values of 15–200 W/m K for bulk CNT samples, including CNT films, CNT ropes, and an aligned CNT array. It should be pointed out that for isolated single CNT involved measurements, heat loss to its surrounding may affect the accuracy of measurement, overestimating its thermal conductivity. In contrast, for bulk CNT samples, heat loss to interair gaps among the tubes could be much smaller than isolated single CNT due to very high CNT number density and very small air gaps among them. The small thermal conductivity for bulk CNT samples may also result from intertube coupling[1,2,6] and high density of defects which efficiently scatter the flow of phonons in CNT's.[5] Further investigation is needed to clarify these issues.

IV. CONCLUSIONS

We have measured the thermal conductivity of MWNT films with film thickness or CNT length from 10 to 50 μm.

The average thermal conductivity is found to be about 15 W/m K and independent of the CNT length. Taking the volume-filling fraction of CNT's into account, the effective thermal conductivity for the MWNT's is about 2×10^{2} W/m K. A comparison between the obtained effective thermal conductivity and electrical conductivity suggests that heat transport in the MWNT's is dominated by phonons. Phonon mean free path is estimated to be 20 nm, much smaller than the CNT length. This is consistent with our observation that the thermal conductivity is independent of CNT length.

[1] Savas Berber, Young-Kyun Kwon, and David Tomanek, Phys. Rev. Lett. **84**, 4613 (2000).

[2] Jianwei Che, Tahir Cagin, and William A. Goddard III, Nanotechnology **11**, 68 (2000).

[3] J. Hone, M. Whitney, C. Piskoti, and A. Zettl, Phys. Rev. B **59**, 2514 (1999).

[4] J. Hone, M. C. Llaguno, N. M. Nemes, A. T. Johnson, J. E. Fischer, D. A. Walters, M. J. Casavant, J. Schmidt, and R. E. Smalley, Appl. Phys. Lett. **77**, 666 (2000).

[5] W. Yi, L. Lu, Zhang Dian-lin, Z. W. Pan, and S. S. Xie, Phys. Rev. B **59**, 9015 (1999).

[6] P. Kim, L. Shi, A. Majumdar, and P. L. McEuen, Phys. Rev. Lett. **87**, 215502 (2001).

[7] A. Mizel, L. X. Benedict, M. L. Cohen, S. G. Louie, A. Zettle, N. K. Budraa, and W. P. Beyermann, Phys. Rev. B **60**, 3264 (1999).

[8] O. M. Corbino, Phys. Z. **11**, 413 (1910).

[9] For Nd:YAG laser operating at 532 nm. The incident light is penetrated over a distance, or skin depth, which is governed by the absorption coefficient of the gold film. The absorption coefficient β can be expressed by $\beta=4\pi n/\lambda$, where n is the imaginary part of the complex refractive index of gold, λ is the optical wavelength. For gold, n is 2.399 at 532 nm. So the skin depth is $1/\beta=17.65$ nm. This value is much less than the thickness of the gold film 1.2 μm.

[10] G. Chen, P. Hui, Thin Solid Films **58**, 339 (1999).

[11] P. Hui and H. S. Tan, IEEE Trans. Compon., Packag. Manuf. Technol., Part. B **17**, No. 3, 426 (1994).

[12] D. L. Balageas, J. C. Kapez, and P. Cielo, J. Appl. Phys. **59**, 348 (1986).

[13] D. Almond, P. Patel, *Photothermal Science and Techniques* (Chapman & Hall, London, 1996).

[14] A. H.-D. Cheng and Y. Abousleiman, Mathematica **4**, 76 (1994).

[15] D. L. Decker, L. G. Koshigoe, and E. J. Ashley, *NBS Special Publication*, Vol. 727, *Laser Induces Damage in Optical Materials* (Government Printing Office, Washington, DC, 1984), p. 291.

[16] J. Hartmann, P. Voigt, and M. Reichling, J. Appl. Phys. **81**, 2966 (1997).

[17] A. Radondo and J. G. Beery, J. Appl. Phys. **60**, 3882 (1986).

[18] E. T. Swartz and R. O. Pohl, Appl. Phys. Lett. **51**, 2200 (1987).

[19] R. F. Speyer, *Thermal Analysis of Materials* (Marcel Dekker, New York, 1994).

[20] L. X. Benedict, S. G. Louie, and M. L. Cohen, Solid State Commun. **100**, 177 (1996).

[21] R. Berman, *Thermal Conduction in Solids* (Oxford University Press, London, 1976).

[22] Shigeo Maruyama (unpublished).